MODERN TRANSISTOR CIRCUITS

John M. Carroll

MODERN TRANSISTOR CIRCUITS

BY JOHN M. CARROLL

MANAGING EDITOR, *Electronics*

McGRAW-HILL BOOK COMPANY, INC.

NEW YORK TORONTO LONDON

1959

preface

TRANSISTORS ARE USED TODAY in nearly every kind of electronic circuit—from portable radios to satellite telemeters. Transistorized equipment is operational, too; not just experimental. Probably the only kind of electronic gear not using transistors in one form or another is high-power transmitters.

All signs point to increasing use of transistors: nearly 10 million were sold in 1956; more than 22 million in 1957. Sales in 1958 ran more than 3.5 million a month. Industry leaders now feel earlier estimates of 450 million transistors a year by 1965 are definitely on the conservative side. All this means that a thorough understanding of transistor circuit design is now an essential part of every electronic engineer's bag-of-tricks.

Reasons for the transistor's ever widening acceptance arise both from better ways of making transistors and better ways of using them. Transistor prices have fallen from $10 or more apiece to, in some cases, less than $.50. The handful of experimental types available in 1952 has grown to upward of 300 commercially available types for every conceivable application: Collector power dissipations range from a few milliwatts to a kilowatt. Alpha cutoff frequencies go from d-c to over 100 megacycles. Modern transistors are noted for their low noise figures as well as small size, low power requirements and absence of warm-up time.

Reliability is one of the most attractive features of present-day transistors. Indeed, their long life and ability to withstand rigorous environments contribute greatly to missile control systems and space satellite communications. Users of transistors now report lifetimes in excess of 10,000 hours. Transistors properly compensated against thermal effects have functioned in equipment subjected to the most extreme temperatures. When properly installed, transistors are practically immune to the effects of shock and vibration.

Several trends in transistor circuit design and device development soon become apparent in preparing a book of this nature. Transistor manufacturers are devoting increasing attention to developing high-frequency units and units that can withstand effectively both extremely high temperatures and high levels of nuclear radiation. Perhaps anticipating a role in control of thermonuclear power.

In circuit design, there are more high-frequency and very-high-frequency transistor circuits, taking advantages of new high-frequency transistors now available. Greater use is being made of complementary symmetry. This circuit configuration was once thought to be of academic interest only, because of difficulties in matching transistor pairs. The trend to complementary symmetry indicates how well transistor manufacturers have improved control over the quality of their products.

Also evident are more hybrid circuits—that is, circuits that use electron tubes and/or magnetic amplifiers as well as transistors. No longer are the supply-voltage-regulation problems and the need to hold chassis temperature down so urgent as to preclude hybrid design. Today the engineer can choose the electron device that best satisfies the needs of the circuit he is currently designing.

A glance at the contents of this book indicates the diverse applications of transistors today. New home-entertainment applications include portable and automobile radio receivers that use fewer parts and do a better job, and miniaturized phonograph preamplifiers. An all-transistor television receiver has been announced.

For the broadcaster there will be sound mixers, wireless microphones and television studio equipment. Communicators will find a large variety of portable transmitters, transceivers, telephone and telegraph terminal equipment. New transistorized instruments include transistor testers, portable frequency meters and extremely small microammeters. New military equipment includes telemetering and missile-guidance equipment, jet engine controls and advanced simulation equipment for training military specialists.

In the fast-growing industrial control field, transistors are doing important work in servo amplifiers, control relays, nuclear reactor controls, metal detectors and measuring instruments.

Transistors are playing an essential role in man's dramatic conquest of outer space. The longest single chapter in this book—28 pages—deals with telemetering circuits for high-speed aircraft, guided missiles and earth satellites. Many other communications, measuring and control circuits presented in other chapters have derived from guided missiles research and development.

Medical electronics is still in its infancy. But the transistor has already become an essential part of telemeters to probe the digestive tract and sensitive amplifiers for diagnostic recording. Transistorized instruments aid scientists in studying ocean currents and behavior of wild life.

The transistor has found a natural niche in the booming computer industry. Both analog and digital computers are using increasing numbers of transistors. Indeed, the transistor's small size alone makes possible computers of a scale thought impracticable only a few years ago. Transistors are also important in analog-to-digital converters and newly designed input/output equipment that may soon permit computers to work at or near their inherently high speeds—not limited to the pace of human or mechanical input and output.

The 101 articles reprinted in this book appeared in *Electronics* magazine during the years 1956, 1957 and 1958. They are published here largely in their entirety. In most cases, circuit schematic diagrams with all component parts values are supplied to short-cut design time. Special thanks are due Bill MacDonald and the staff of *Electronics* magazine whose skill and editorial judgment have made possible the timeliness, scope and completeness of this material.

John M. Carroll

contents

CIRCUIT DESIGN DATA

HOW TRANSISTORS OPERATE UNDER ATOMIC RADIATION

By ROBERT L. RIDDLE
Senior Engineer, Haller, Raymond and Brown, Inc., State College, Pa.

Results of tests exposing transistor amplifier and single transistor to radiation from nuclear reactor show that degrading effects of irradiation can be controlled to some degree by use of negative feedback when applicable. Radiation effects on coaxial cables showed no noticeable change in r-f transmission characteristics

APPLICATION of nuclear energy to propulsion of ships, planes and other devices will require electronic equipment to operate under a wide range of nuclear radiation levels. For circuits to function properly, it will be necessary for designers to compensate for irradiation effects on active circuit elements.

Investigations have been made to find the effects of combined gamma and neutron flux on semiconductor devices. The facilities of the Pennsylvania State University pool-type research reactor were used for an experiment involving the effects of reactor radiation on an all-transistor amplifier and crystal video detector. Arrangement of the test is shown in block form in Fig. 1A.

Test Method

In general, the information desired was the overall performance of the combined crystal detector and transistor amplifier shown in Fig. 1B. Measurements included tangential sensitivity and transfer ratio of the system (ratio of video output voltage to r-f input voltage). Also determined were r-f attenuation in a coaxial cable extending from the center of the active pile area to the top of the pool and the *h*-parameters and I_{co} measurements on a single separate transistor in the active pile area. Noise in a properly terminated coaxial cable in the active area was also measured.

The tangential sensitivity was determined under the conditions of a 1,000-mc carrier pulsed by 10-

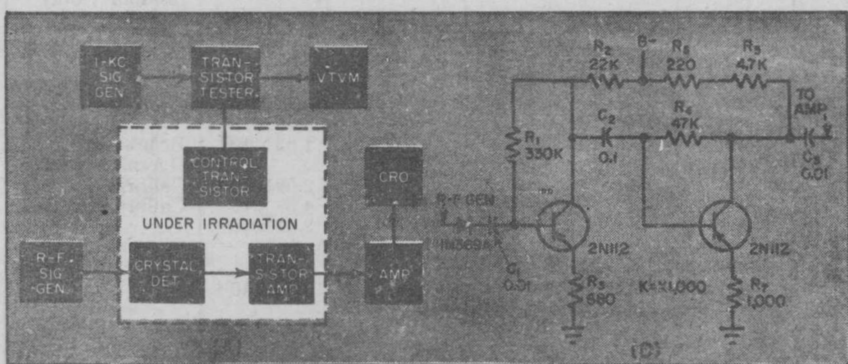

FIG. 1—Equipment setup used in irradiation study (A) with circuit of detector and transistor amplifier (B)

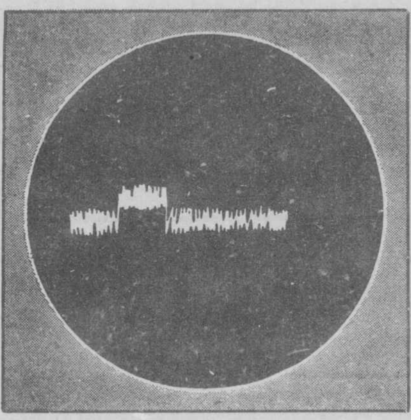

FIG. 2—Oscilloscope pattern used in determination of tangential sensitivity

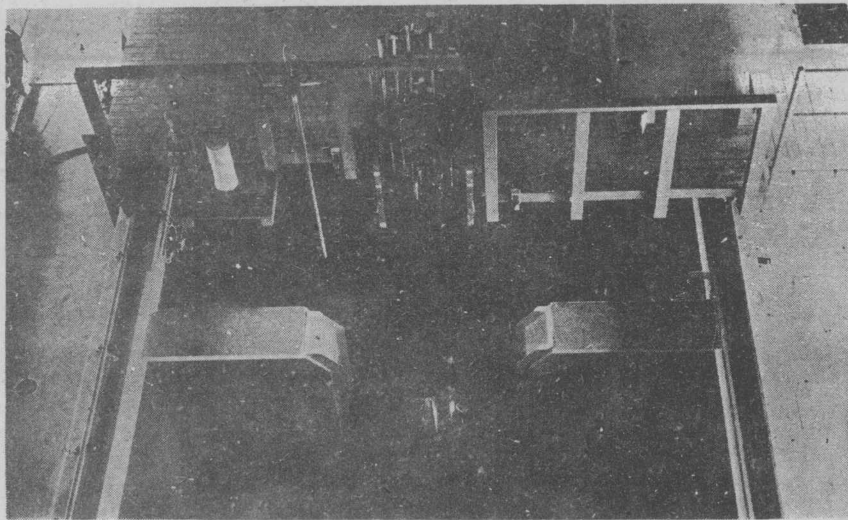

Pool-type reactor. Amplifier was placed in aluminum tube for insertion in reactor

microsecond rectangular pulses at 5,000 pps. The tangential sensitivity was measured by adjusting power level so that on an oscilloscope pattern the bottom of the noise during the pulse was even with the top of the noise when the pulse was absent. A typical pattern is shown in Fig. 2. The power level input when such a picture is obtained is the tangential sensitivity.

The determination of the transfer ratio was made from the calibrated attenuator on the signal generator and a calibrated oscilloscope.

The control measurements were included so that the primary effects of radiation on the amplifier-detector system could be separated from possible extraneous effects.

The irradiation schedule is shown in Table I with irradiation times listed for each power level. Neutron flux ϕ, in neutrons per cm²-sec, is the combined thermal and resonance flux as determined by a cadmium ratio of 9.4 and $\phi_{thermal} = 2.07 \times 10^6 \times P$ as found by activation of foils. This gives $\phi = 2.32 \times 10^6 \times P$, where P is the reactor power in watts. Total flux ϕ includes approximately those neutrons between thermal energies and 2 ev.

The duration of each test in seconds and the integrated neutron flux is also given in the table. Gamma dose was determined from previous calibrations to be equivalent to a dose in roentgens per hour of $4.93 \times 10\ P$. The gamma dose shown in the table is calculated from this equation. The integrated gamma dose was $3.2 \times 10^6 R$.

Table I—Exposure Time for Transistors in Reactor

Test No.	Power in watts	ϕ in Neutrons per cm²-sec	γ flux in γ/hr	Test duration in sec	Integrated flux density in neutrons per cm²	Remarks
1	0	0	>100		0	Zero power, residual γ only
2	0.3	0.7×10^6	300	420	2.9×10^8	
3	10	2.3×10^7	793	840	1.95×10^{10}	
4	10^2	2.3×10^8	4.9×10^3	540	1.25×10^{11}	
5	10^3	2.3×10^8	4.9×10^4	420	9.75×10^{11}	
6	10^4	2.3×10^{10}	4.9×10^5	420	9.75×10^{12}	
7	5×10^4	1.16×10^{11}	2.5×10^6	480	5.56×10^{13}	
8	10^2	2.3×10^8	$\cong5\times10^3$	660	1.53×10^{11}	Reactor off
9	Reactor off	....	$\cong300$	58,440		Overnight decay
—	10^2	2.3×10^3	4.9×10^3	900	2.09×10^{11}	Calibrate
—	0 13	3.1×10^5	$\cong300$	14,280	4.3×10^9	Calibrate & off
10	10^4	2.3×10^{10}	4.9×10^5	1,020	2.37×10^{13}	
11	10^5	2.3×10^{11}	4.9×10^6			
12	10^5	2.3×10^{11}	4.9×10^6			
13	10^5	2.3×10^{11}	4.9×10^6	1,920	4.46×10^{14}	
14	10^5	2.3×10^{11}	4.9×10^6			
15	0	0	0	840	0	**Pulled sample out of aluminum tube**
16	0	0	0	1,020	0	
17	0	0	0	63,360	0	

Test Results

The results of this experiment are shown in Fig. 3. The tangential sensitivity, the most important measurement on a crystal video system, is shown in Fig. 3A and Fig. 3B. Sensitivity decreased as the experiment progressed. There is a recovery in sensitivity as soon as the reactor is turned off as shown by tests 7 and 8. Test 9, which was performed several hours later, still shows about the same sensitivity.

Upon turning the reactor on again, the sensitivity again decreased with increasing flux. The recovery after removing the apparatus from the flux field, represented by test 15, is not as pronounced as that of test 8. Slight improvement is noticed, however, several hours later.

The results of this test show that the sensitivity is affected by flux density as well as integrated flux. The dashed line represents a guess at the probable effects of integrated flux, and the solid line the actual measurements which represent a combination of permanent and temporary effects. The distance between the solid line and dashed line approximates the effects of the temporary degradation as a result of the flux density. This is indicated by the amount of effective

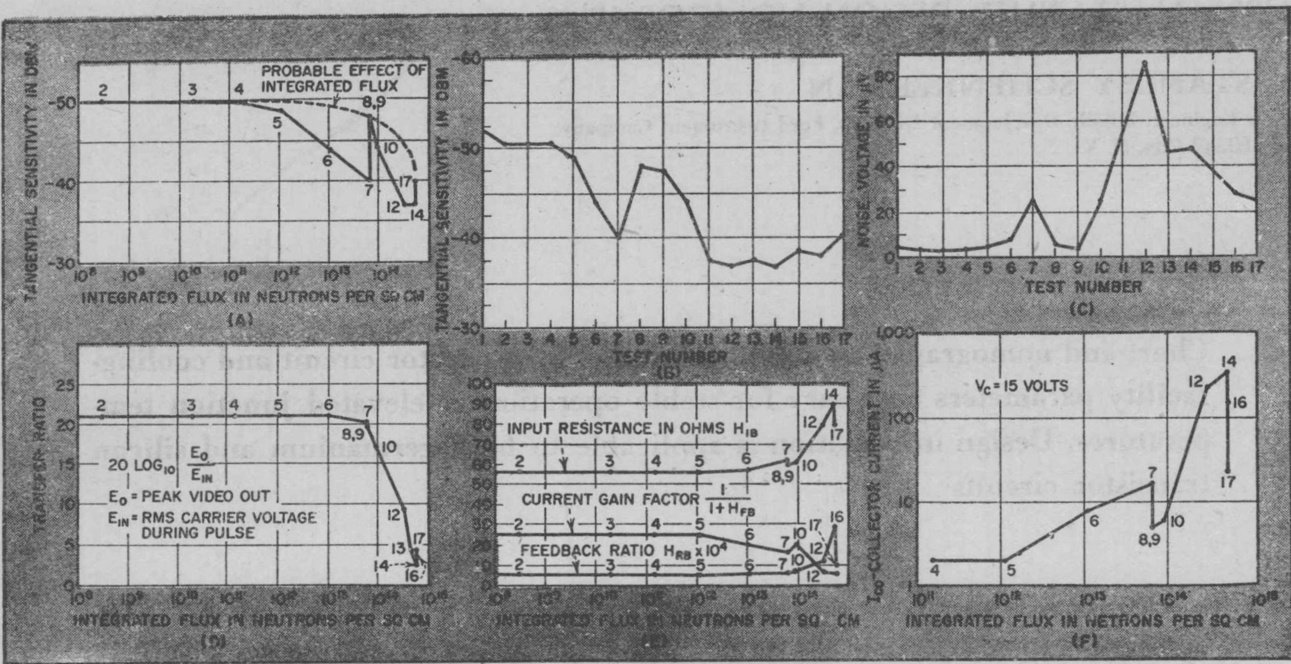

FIG. 3—Results of irradiation study shown graphically are described in text. Numbers on chart indicate test

noise voltage present at the input to the crystal shown in Fig. 3C. This noise voltage is large in those tests where flux density is large. The presence of this noise at these high flux levels results in the decreased tangential sensitivity shown in Fig. 3A and Fig. 3B.

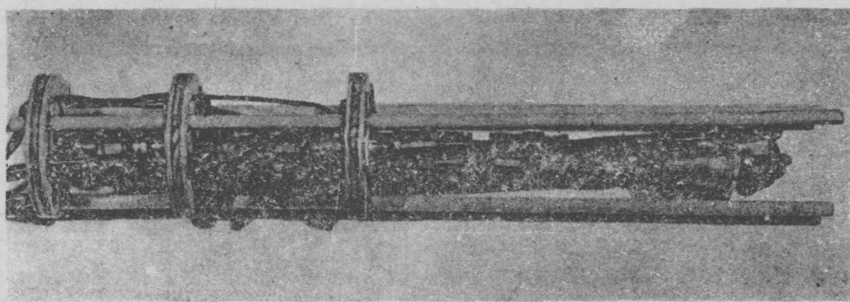

Transistor amplifier used in test is slipped into aluminum pipe to center of reactor

Transfer Ratio

The transfer ratio, measured as the peak-to-peak pulse output to the rms r-f input, is shown in Fig. 3D. No degradation in this ratio took place until an integrated neutron flux in excess of 10^{13} neutrons per sq cm was reached. From this point on, the transfer ratio dropped rapidly as the integrated flux increased. This same general trend is represented in Fig. 3E which shows the effect on the parameters of the control transistor. This transistor started to degrade at an integrated flux of slightly larger than 10^{12} neutrons per sq cm.

The crystal video circuit maintained its gain for an order of magnitude longer. This is probably a result of the degeneration present in the circuit. The transfer ratio recovered slightly after the device was taken from the flux field. This recovery was gradual and may possibly be due to thermal annealing of the defects produced by irradiation. This same effect is noticed in the control transistor parameters.

The I_{co} of the control transistor was also monitored throughout the test and variation is shown in Fig. 3F. The increase in I_{co} may be in part due to internal gamma heating in the transistor.

There was no noticeable change in the r-f transmission through the coaxial cable used as a control. This cable was not monitored for attenuation of video signals.

The noise power produced in a 12-mc bandwidth by the properly terminated cable was −84 dbm residual. The maximum reading on this cable was −82 dbm. This is well below the level of the r-f signal used in the test and also was measured in a much broader bandwidth than that of the crystal detector and transistor amplifier.

Several conclusions may be drawn from this experiment. Fission spectrum irradiation upon semiconductor devices has essentially three effects. These are transient effects resulting from flux density and gamma heating, semipermanent effects resulting from integrated flux and permanent effects resulting from integrated flux after annealing.

The transient effects caused by flux density are effective mainly in producing noise and increasing I_{co}. The gamma heating, the second transient effect, appears to increase I_{co} and degrades the transistor in the same manner as any increase in temperature. These effects disappear soon after removal from the flux field.

The semipermanent effects caused by integrated flux result from lattice damage and transmutations. The semipermanent damage results in an overall change in the characteristics of the semiconductor devices which usually degrade their operation.

THERMAL STABILITY DESIGN NOMOGRAPHS

By STANLEY SCHENKERMAN

Senior Engineer, Missile Development Division, Ford Instrument Company, Long Island City, N. Y.

Chart and nomographs simplify calculation of transistor circuit and cooling-facility parameters necessary for stable operation at elevated junction temperatures. Design information is applicable to both germanium and silicon transistor circuits

TO ACHIEVE THERMAL STABILITY of transistorized equipment at elevated junction temperatures, the designer must provide a circuit compatible with its cooling facility. The accompanying graph and nomographs permit the rapid determination of suitable circuit and cooling facility parameters.

Theory

The thermal stability nomograph, Fig. 1, is based upon the criteria for thermal stability[1]

$$SV_cI_s\theta < 13 \qquad (1A)$$

for germanium and

$$SV_cI_s\theta < 23 \qquad (1B)$$

for silcon.

The stability factor[2] S is the change in quiescent collector current caused by a change in the temperature sensitive component, V_c is collector voltage, I_s is the temperature sensitive component of collector current and cooling-facility characteristic θ is the thermal resistance from collector junction to ambient in deg C per watt. The designer's objective is to obtain compatible values of S and θ.

Temperature sensitive current I_s increases exponentially with temperature, doubling every 9 C for germanium and every 16 C for silicon. The value of I_s at any temperature T may be found from Fig. 2 if the value of I_{so} at any temperature T_o is known; the latter values can be obtained from the manufacturer's data sheet.

Thermal resistance θ consists of the resistance from collector junction to mounting base, θ_{jm}, (specified by the manufacturer) and the resistance from mounting base to ambient, θ_{ma}. The latter may be determined experimentally from

$$\theta_{ma} = \Delta T/P_d \qquad (2)$$

where ΔT is the mounting base temperature rise above ambient in degrees centigrade and P_d is the transistor dissipation in watts. Then

$$\theta = \theta_{ma} + \theta_{jm}. \qquad (3)$$

The thermal resistance nomo-

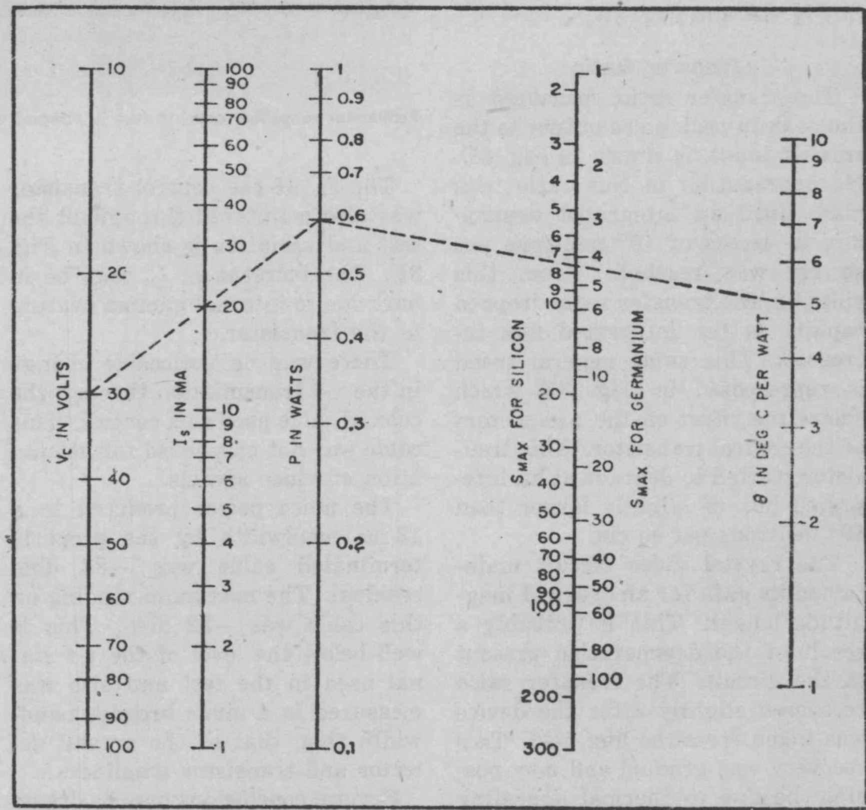

FIG. 1—Range of thermal stability nomograph is extended by powers of 10

graph, Fig. 3, facilitates the solution of Eq. 2 and 3.

From measurements, it is determined that at 4 w dissipation, the mounting base temperature of a transistor, when installed in the cooling facility, is 8 C. The resistance from junction to mounting base is specified as 3 C per watt.

Thermal Resistance

Using Fig. 3, connect the point $\Delta T = 8$ C with the point $P_d = 4$ w with a straight line that intersects $\theta_{ma} = 2$ C per watt. Next, connect $\theta_{ma} = 2$ C per watt and $\theta_{jm} = 3$ C per watt with a straight line. This line intersects $\theta = 5$ C per watt which is the total thermal resistance of the cooling facility.

The value of S_{max} may now be found from the thermal stability nomograph of Fig. 1. The circuit S must be less than S_{max} for stability. Conversely, for a given S the maximum permissible θ may be determined.

The transistor of the previous example is a germanium unit with $I_{so} = 0.2$ ma at $T_o = 25$ C. It is desired to operate this unit with $V_c = 30$ v at 85 C in the cooling facility for which $\theta = 5$ C per watt. Since $T - T_o$ is 60 C, I_s/I_{so} is 100 as determined from Fig. 2. Then I_s is 20 ma at 85 C.

On the stability nomograph, Fig. 1, connect $V_c = 30$ and $I_s = 20$ with a straight line that intersects the P scale at 0.6. Now connect this point by a straight line with $\theta = 5$. This line intersects S_{max} for germanium at 4.3. This is the maximum value of S for which the circuit is thermally stable.

REFERENCES

(1) Specification for H-5, H-6, and H-7 Power Transistors, Transistor Div., Minneapolis Honeywell Regulator Co., p 9, May 1956.

(2) R. F. Shea, "Principles of Transistor Circuits", John Wiley Sons, Inc., p 97, 1953.

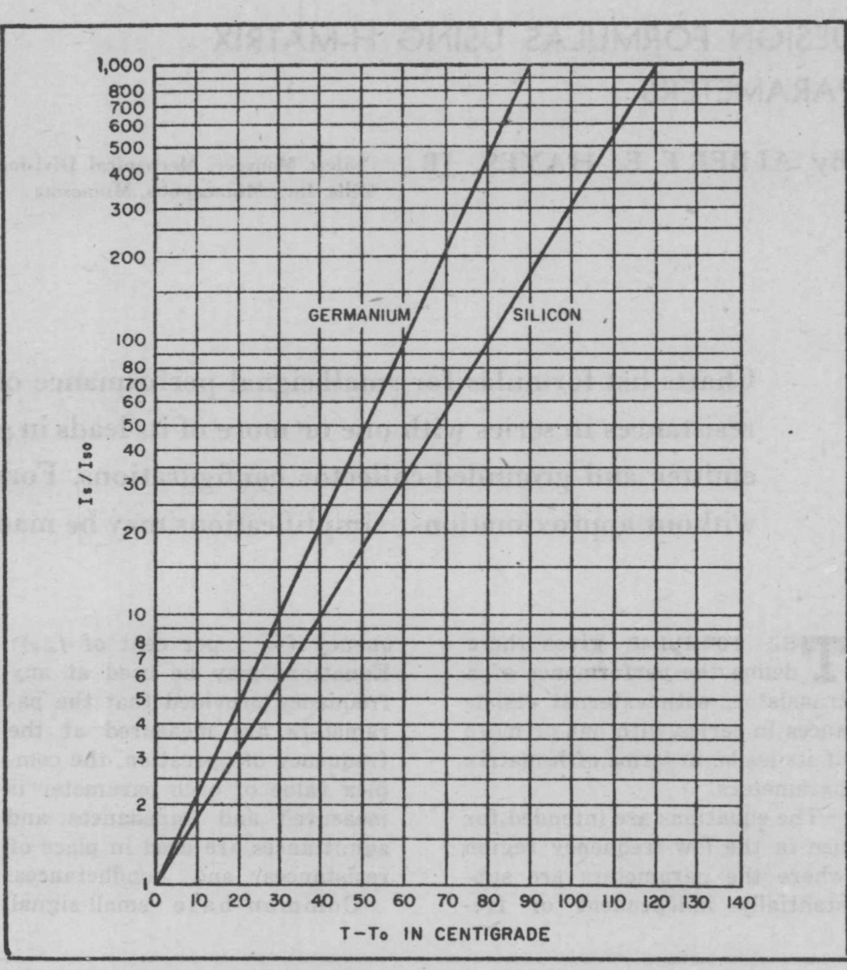

FIG. 2—Curves give normalized temperature-sensitive leakage current as function of temperature change

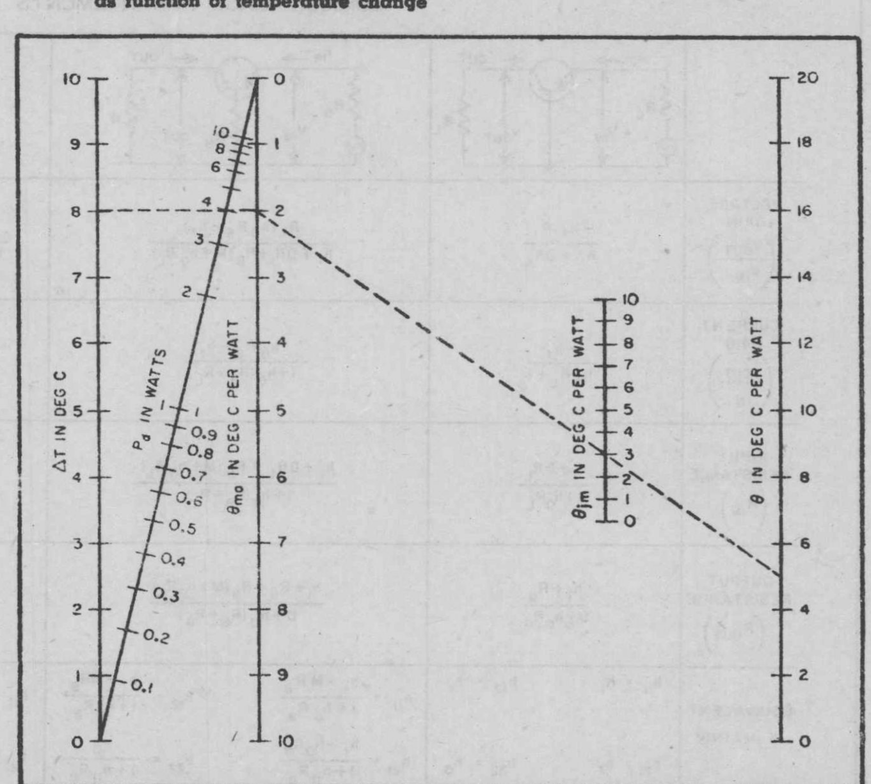

FIG. 3—Range of thermal resistance nomograph is extended by powers of 10

DESIGN FORMULAS USING H-MATRIX PARAMETERS

By ALBERT E. HAYES, JR. Project Manager, Mechanical Division, General Mills, Inc., Minneapolis, Minnesota

Charts list formulas for small-signal performance of transistor with external resistances in series with one or more of its leads in grounded-base, grounded-emitter and grounded-collector configurations. Formulas have been derived without approximations; simplifications may be made to fit specific situations

THE FORMULAS given here define the performance of a transistor, with external resistances in series with one or more of its leads, in terms of h-matrix parameters.

The equations are intended for use in the low-frequency region where the parameters are substantially independent of frequency ($\approx$ 1 per cent of $f_{\alpha o}$). Equations may be used at any frequency provided that the parameters are measured at the frequency of operation, the complex value of each parameter is measured and impedances and admittances are used in place of resistances and conductances.

Common-base small-signal, short-circuit input resistance is designated by h_i, open-circuit reverse-transfer voltage ratio by h_r, short-circuit forward-transfer current ratio by h_f and open-circuit output conductance by h_o. Quantity D is the determinant of the h matrix ($D = h_i h_o - h_f h_r$), and $M = D + h_f - h_r + 1$.

COMMON-BASE ARRANGEMENTS

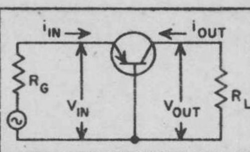

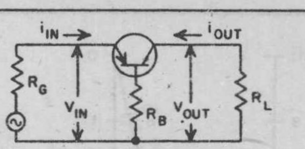

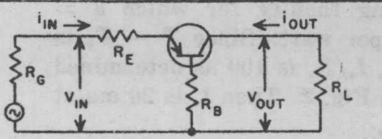

VOLTAGE GAIN $\left(\frac{V_{OUT}}{V_{IN}}\right)$	$\frac{-h_f R_L}{h_i + DR_L}$	$\frac{R_L(h_O R_B - h_f)}{h_i + DR_L + R_B(M + h_O R_L)}$	$\frac{R_L(h_O R_B - h_f)}{h_i + DR_L + R_B(M + h_O R_L + h_O R_E) + R_E(1 + h_O R_L)}$
CURRENT GAIN $\left(\frac{i_{OUT}}{i_{IN}}\right)$	$\frac{-h_f}{h_O R_L + 1}$	$\frac{h_O R_B - h_f}{1 + h_O(R_B + R_L)}$	$\frac{h_O R_B - h_f}{1 + h_O(R_B + R_L)}$
INPUT RESISTANCE (R_{IN})	$\frac{h_i + DR_L}{1 + h_O R_L}$	$\frac{h_i + DR_L + R_B(M + h_O R_L)}{1 + h_O(R_B + R_L)}$	$R_E + \frac{h_i + DR_L + R_B(M + h_O R_L)}{1 + h_O(R_B + R_L)}$
OUTPUT RESISTANCE (R_{OUT})	$\frac{h_i + R_G}{D + h_O R_G}$	$\frac{h_i + R_G + R_B(M + h_O R_G)}{D + h_O(R_B + R_G)}$	$\frac{h_i + R_G + R_E + R_B[M + h_O(R_G + R_E)]}{D + h_O(R_B + R_E + R_G)}$
EQUIVALENT h MATRIX	$h_{11} = h_i$ $h_{12} = h_r$ $h_{21} = h_f$ $h_{22} = h_O$	$h_{11} = \frac{h_i + MR_B}{1 + h_O R_B}$ $h_{12} = \frac{h_r + MR_B}{1 + h_O R_B}$ $h_{21} = \frac{h_f - h_O R_B}{1 + h_O R_B}$ $h_{22} = \frac{h_O}{1 + h_O R_B}$	$h_{11} = R_E + \frac{h_i + MR_B}{1 + h_O R_B}$ $h_{12} = \frac{h_r + h_O R_B}{1 + h_O R_B}$ $h_{21} = \frac{h_f - h_O R_B}{1 + h_O R_B}$ $h_{22} = \frac{h_O}{1 + h_O R_B}$

COMMON-EMITTER ARRANGEMENTS

	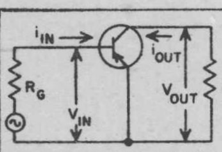	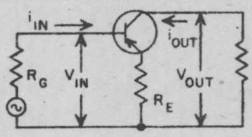	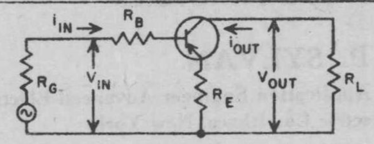
VOLTAGE GAIN $\left(\frac{V_{OUT}}{V_{IN}}\right)$	$\frac{(D+h_f)R_L}{h_i+DR_L}$	$\frac{(D+h_f+h_oR_E)R_L}{h_i+DR_L+R_E(1+h_oR_L)}$	$\frac{(D+h_f+h_oR_E)R_L}{h_i+DR_L+R_E[1+h_o(R_B+R_L)]+R_B(M+h_oR_L)}$
CURRENT GAIN $\left(\frac{i_{OUT}}{i_{IN}}\right)$	$\frac{D+h_f}{h_oR_L+M}$	$\frac{D+h_f+h_oR_E}{h_o(R_E+R_L)+M}$	$\frac{D+h_f+h_oR_E}{h_o(R_E+R_L)+M}$
INPUT RESISTANCE (R_{IN})	$\frac{DR_L+h_i}{h_oR_L+M}$	$\frac{DR_L+h_i+R_E(1+h_oR_L)}{h_o(R_E+R_L)+M}$	$R_B+\frac{DR_L+h_i+R_E(1+h_oR_L)}{h_o(R_E+R_L)+M}$
OUTPUT RESISTANCE (R_{OUT})	$\frac{h_i+MR_G}{D+h_oR_G}$	$\frac{h_i+MR_G+R_E(1+h_oR_G)}{D+h_o(R_E+R_G)}$	$\frac{h_i+M(R_B+R_G)+R_E[1+h_o(R_B+R_G)]}{D+h_o(R_B+R_E+R_G)}$
EQUIVALENT h MATRIX	$h_{11}=\frac{h_i}{M}$ $h_{12}=\frac{D-h_r}{M}$ $h_{21}=\frac{-(D+h_f)}{M}$ $h_{22}=\frac{h_o}{M}$	$h_{11}=\frac{h_i+R_E}{M+h_oR_E}$ $h_{12}=\frac{D-h_r+h_oR_E}{M+h_oR_E}$ $h_{21}=\frac{-(D+h_f+h_oR_E)}{M+h_oR_E}$ $h_{22}=\frac{h_o}{M+h_oR_E}$	$h_{11}=R_B+\frac{h_i+R_E}{M+h_oR_E}$ $h_{12}=\frac{D-h_r+h_oR_E}{M+h_oR_E}$ $h_{21}=\frac{-(D+h_f+h_oR_E)}{M+h_oR_E}$ $h_{22}=\frac{h_o}{M+h_oR_E}$

COMMON-COLLECTOR ARRANGEMENTS

	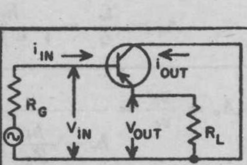	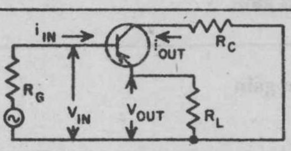	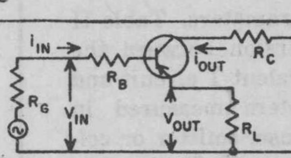
VOLTAGE GAIN $\left(\frac{V_{OUT}}{V_{IN}}\right)$	$\frac{(1-h_r)R_L}{h_i+R_L}$	$\frac{(1-h_r+h_oR_C)R_L}{h_i+R_L(1+h_oR_C)+DR_C}$	$\frac{(1-h_r+h_oR_C)R_L}{h_i+DR_C+R_L[1+h_o(R_B+R_C)]+R_B(M+h_oR_C)}$
CURRENT GAIN $\left(\frac{i_{OUT}}{i_{IN}}\right)$	$\frac{1-h_r}{h_oR_L+M}$	$\frac{1-h_r+h_oR_C}{h_o(R_C+R_L)+M}$	$\frac{1-h_r+h_oR_C}{h_o(R_C+R_L)+M}$
INPUT RESISTANCE (R_{IN})	$\frac{h_i+R_L}{h_oR_L+M}$	$\frac{h_i+R_L+R_C(D+h_oR_L)}{h_o(R_C+R_L)+M}$	$R_B+\frac{h_i+R_L+R_C(D+h_oR_L)}{h_o(R_C+R_L)+M}$
OUTPUT RESISTANCE (R_{OUT})	$\frac{h_i+MR_G}{1+h_oR_G}$	$\frac{h_i+MR_G+R_C(D+h_oR_G)}{1+h_o(R_C+R_G)}$	$\frac{h_i+(M+h_oR_C)(R_B+R_G)+DR_C}{1+h_o(R_B+R_C+R_G)}$
EQUIVALENT h MATRIX	$h_{11}=\frac{h_i}{M}$ $h_{12}=\frac{1+h_f}{M}$ $h_{21}=\frac{h_r-1}{M}$ $h_{22}=\frac{h_o}{M}$	$h_{11}=\frac{h_i+DR_C}{M+h_oR_C}$ $h_{12}=\frac{1+h_f+h_oR_C}{M+h_oR_C}$ $h_{21}=\frac{h_r-1-h_oR_C}{M+h_oR_C}$ $h_{22}=\frac{h_o}{M+h_oR_C}$	$h_{11}=R_B+\frac{h_i+DR_C}{M+h_oR_C}$ $h_{12}=\frac{1+h_f+h_oR_C}{M+h_oR_C}$ $h_{21}=\frac{h_r-1-h_oR_C}{M+h_oR_C}$ $h_{22}=\frac{h_o}{M+h_oR_C}$